AGU PUBLICATIONS

Geophysical Research Letters

RESEARCH LETTER
10.1002/2014GL060004

Key Points:
- Tropical land carbon-climate sensitivity in ESMs from CMIP5 are investigated
- A weak linear relationship exists between climate impact and CO_2 sensitivity
- The uncertainty of climate impact in the CMIP5 ESMs can barely be reduced

Supporting Information:
- Readme
- Figure S1
- Table S1

Correspondence to:
N. Zeng and Q. Bao,
zeng@atmos.umd.edu;
baoqing@lasg.iap.ac.cn

Citation:
Wang, J., N. Zeng, Y. Liu, and Q. Bao (2014), To what extent can interannual CO_2 variability constrain carbon cycle sensitivity to climate change in CMIP5 Earth System Models?, *Geophys. Res. Lett.*, *41*, doi:10.1002/2014GL060004.

Received 25 MAR 2014
Accepted 27 APR 2014
Accepted article online 30 APR 2014

To what extent can interannual CO_2 variability constrain carbon cycle sensitivity to climate change in CMIP5 Earth System Models?

Jun Wang[1,2], Ning Zeng[3], Yimin Liu[1], and Qing Bao[1]

[1]State Key Laboratory of Numerical Modelling for Atmospheric Sciences and Geophysical Fluid Dynamics, Institute of Atmospheric Physics, Beijing, China, [2]University of Chinese Academy of Sciences, Beijing, China, [3]Department of Atmospheric and Oceanic Science and Earth System Science Interdisciplinary Center, University of Maryland, College Park, Maryland, USA

Abstract We analyze the carbon-climate feedback in eight Earth System Models from phase 5 of the Coupled Model Intercomparison Project (CMIP5). We focus on tropical land carbon change and find decreases (-31.02 to -169.32 GtC K^{-1}) indicating tropical ecosystems will release carbon as temperature warms, thus contributing to a positive feedback identified in earlier studies. We further investigate the relationship between tropical land carbon change and sensitivity of historical atmospheric CO_2 growth rate to tropical temperature variability and find a weak linear relationship. This sensitivity for most models is stronger than observed. We further use this "emergent constraint" to constrain uncertainties in model-projected future carbon-climate changes and find little effect in narrowing the model spread, but the mean sensitivity is slightly smaller. This contrasts with earlier Coupled Carbon Cycle Climate Model Intercomparison Project results, highlighting the challenge in constraining future projections by modern observations and the necessity for evaluating such relationships continuously.

1. Introduction

The terrestrial ecosystem will exert a positive feedback effect on future global warming [*Cox et al.*, 2000; *Dufresne et al.*, 2002; *Zeng et al.*, 2004; *Friedlingstein et al.*, 2006]. The land carbon sink will be affected by the elevated atmospheric CO_2 concentration and the changes in temperature and other climate elements. *Friedlingstein et al.* [2006] found that carbon-climate feedback is positive in all the 11 models of the Coupled Carbon Cycle Climate Model Intercomparison Project (C^4MIP), albeit with a large spread. This feedback is largely attributed to the changes in photosynthesis, respiration, and demographic processes that influence the carbon residence time in vegetation [*Friend et al.*, 2014], but the relative roles of different processes vary greatly from model to model. One major factor is the sensitivity of land carbon to temperature increase [*Booth et al.*, 2012]. The majority of the coupled carbon cycle models in C^4MIP simulate a reduction of land carbon sequestration over the tropics [*Friedlingstein et al.*, 2006]. *Cox et al.* [2004] projected the Amazonian forest dieback for the 21st century, induced by warming and drought. However, recent simulations indicated much lower risk of dieback from the Amazonian rainforests [*Huntingford et al.*, 2013], but increased tree mortality in response to severe drought in 2005 and 2010 is occurring [*Marengo et al.*, 2008, 2011; *Zeng et al.*, 2008; *Phillips et al.*, 2009]. In the most recent phase 5 of the Coupled Model Intercomparison Project (CMIP5), the level of uncertainty in the carbon cycle appears not to have been reduced [*Friedlingstein et al.*, 2013; *Shao et al.*, 2013; *Hoffman et al.*, 2014]. Thus, it is critically important to use modern and past observations to constrain the carbon-climate uncertainty [*Cox et al.*, 2013; *Hoffman et al.*, 2014].

In an elegant statistical analysis, *Cox et al.* [2013] used the observed historical sensitivity of the atmospheric CO_2 growth rate to tropical temperature variability [*Bacastow*, 1976] to constrain the uncertainty of the tropical land climate impact. Using results from six fully coupled carbon-climate models from the C^4MIP project, they found a remarkable linear relationship between the simulated historical sensitivity of the CO_2 growth rate and the sensitivity of tropical land carbon sequestration to tropical temperature warming. They were then able to use this linear relationship in a Bayesian framework to narrow the uncertainty range in these models' future projections.

Here we apply a similar approach to investigate the sensitivity of tropical land carbon sequestration to tropical temperature warming and the sensitivity of the historical atmospheric CO_2 growth rate to tropical

temperature interannual variability (IAV) but through using eight Earth System Models (ESMs) involved in CMIP5. The model simulations we use are the emissions-driven fully coupled and ideal concentration-driven biogeochemical coupled runs. Our main goal is to test to what degree modern observations of CO_2 variability can be used to constrain future carbon-climate feedback, in particular how such capability depends on model choice.

2. Models and Methodology

2.1. ESMs in CMIP5

We use eight available ESMs in CMIP5 to make this analysis. The components of the carbon cycle and their resolutions are summarized in Table S1 in the supporting information. The names of the ESMs are as follows: (1) bcc-csm1.1 (Beijing Climate Center) [*Wu et al.*, 2013]; (2) CanESM2 (Canadian Center for Climate Modeling and Analysis) [*Arora et al.*, 2011]; (3) CESM1-BGC (National Center for Atmospheric Research) [*Hurrell et al.*, 2013; *Keppel-Aleks et al.*, 2013]; (4) FGOALS-s2 (Institute of Atmospheric Physics) [*Bao et al.*, 2013; *Wang et al.*, 2013]; (5) GFDL-ESM2M (NOAA Geophysical Fluid Dynamics Laboratory) [*Dunne et al.*, 2013]; (6) HadGEM2-ES (Met Office Hadley Center) [*Collins et al.*, 2011; *Jones et al.*, 2011]; (7) MPI-ESM-LR (Max Planck Institute for Meteorology) [*Ilyina et al.*, 2013]; and (8) NorESM1-ME (Norwegian Climate Center) [*Tjiputra et al.*, 2012].

2.2. Approaches for the Carbon-Climate and Carbon Concentration Feedback Parameters

Following previous studies [*Friedlingstein et al.*, 2003, 2006], a linear assumption is made to infer the dependences of tropical land carbon change on the change of atmospheric CO_2 and of tropical mean temperature. We obtain the carbon concentration and carbon-climate feedback parameters based on two experiments in CMIP5 [*Taylor et al.*, 2012]: (1) the fully coupled run forced by prescribed anthropogenic emissions with historical CO_2 emissions of fossil fuels [*Andres et al.*, 2011] and land use change [*Houghton*, 2010] as well as 21st century emissions for the representative concentration pathway 8.5 (RCP8.5) [*Riahi et al.*, 2007] and (2) the biogeochemical coupled run with the carbon cycle forced by CO_2 at a rate of a 1% increase per year from the preindustrial value (284.725 ppm) to 4 times that value, but the radiation code sees a time-invariant preindustrial CO_2 concentration. The formulae are written as follows:

1. Fully coupled run

$$\delta H^{*} = \beta \delta \mathrm{CO}_2^{*} + \gamma \delta T^{*}; \tag{1}$$

2. Biogeochemical coupled run

$$\delta H^{+} = \beta \delta \mathrm{CO}_2^{+} + \gamma \delta T^{+}, \tag{2}$$

where δH^{*} and δH^{+} denote the changes of the tropical land carbon storage (30°S–30°N) in the fully coupled run from 1960 to 2099 and the biogeochemical coupled run from model year 1 to 140, respectively. $\delta \mathrm{CO}_2^{*}$ and $\delta \mathrm{CO}_2^{+}$ denote the changes of the atmospheric CO_2 concentration, and δT^{*} and δH^{+} represent the changes of the tropical mean temperature in the two runs. Because there is no radiative forcing in the biogeochemical coupled run, the temperature change (δH^{+}) is small but not 0. This small temperature change can be attributed to the change of vegetation structure and distribution along with the atmospheric CO_2 increase. β and γ are the sensitivities of tropical land carbon sequestration to atmospheric CO_2 effects and to climate change, respectively. Assuming they hold constant in the two kinds of coupled runs, we can deduce their values.

2.3. Anomalies of the Atmospheric CO_2 Growth Rate and Tropical Mean Temperature

We take the combination of the globally averaged marine surface annual mean CO_2 data from National Oceanic and Atmospheric Administration (NOAA)/Earth System Research Laboratory (www.esrl.noaa.gov/gmd/ccgg/trends/) for 1980 to 2010 and the historical data sets from the RCP scenarios [*Meinshausen et al.*, 2011] for 1960 to 1979 as the observed CO_2 concentration. The atmospheric CO_2 growth rates of the observation and ESM simulations are calculated as

$$\left.\frac{\mathrm{dCO_2}}{\mathrm{d}t}\right|_n = \mathrm{CO_2}(n) - \mathrm{CO_2}(n-1), \tag{3}$$

where n denotes the nth year.

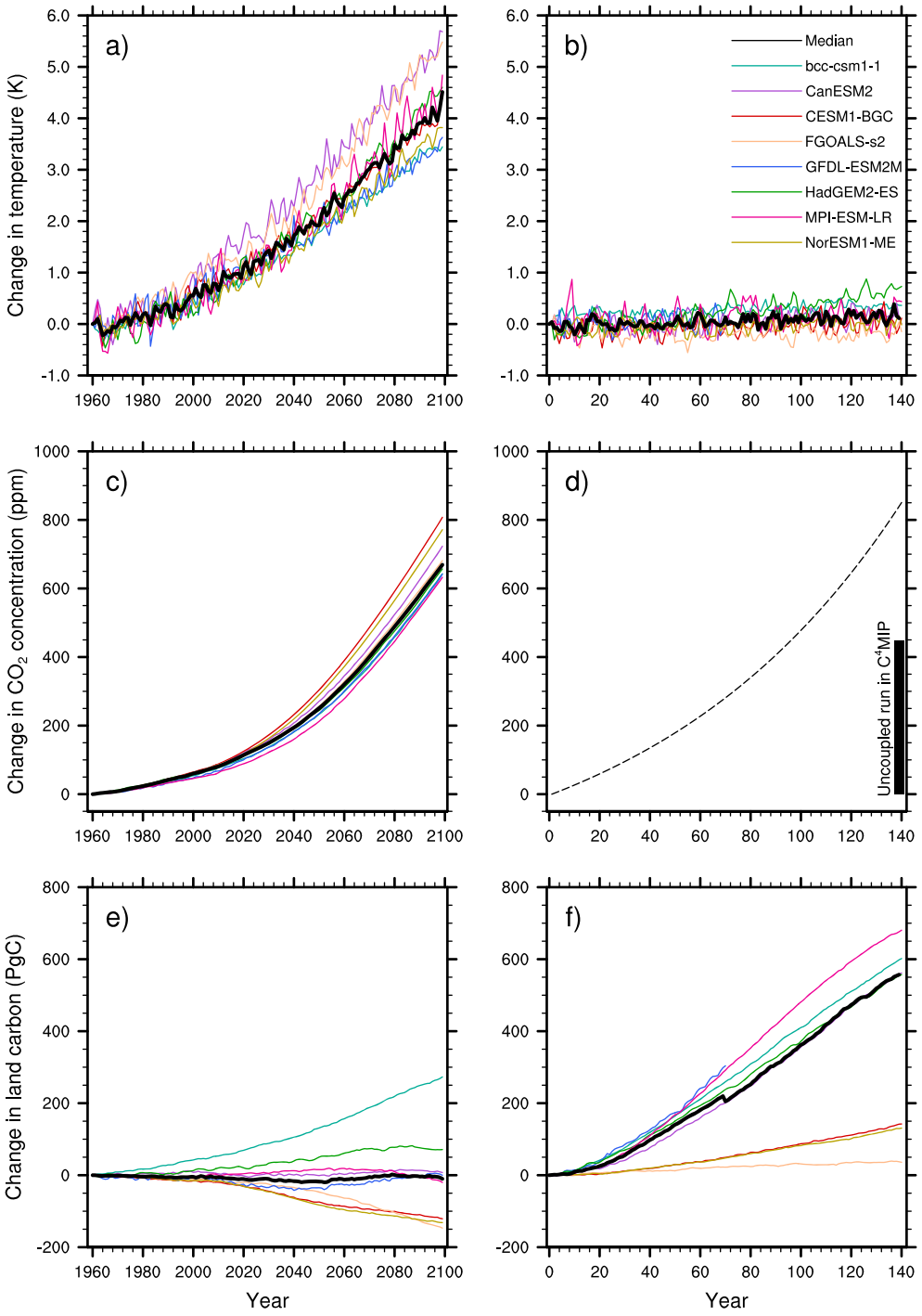

Figure 1. Changes of tropical near-surface air temperature, tropical land carbon pools (30°S–30°N), and atmospheric CO_2 concentration, simulated by eight Earth System Models (ESMs) participating in CMIP5, in the (a, c, e) fully coupled and (b, d, f) biogeochemical coupled runs, respectively. The carbon cycle in the biogeochemical run is forced by the atmospheric CO_2 concentration at a rate of 1% increase per year from the preindustrial value (284.725 ppm) to 4 times the initial concentration, so Figure 1d only presents one curve demonstrating the ideal change of the CO_2 concentration. And the black bar in Figure 1d shows the mean CO_2 concentration change in C^4MIP models for the uncoupled run from 1960 to 2099 [*Cox et al.*, 2013]. The GFDL-ESM2M model increases its CO_2 only to the double (70 years) according to its experimental design, and we take the first 70 years to make the analysis (blue curve in Figures 1b and 1f). In all but Figure 1d, the black curve shows the median value.

Table 1. Changes of Physical Variables in the Climate-Carbon Cycle Projections[a]

	Biogeochemical Coupled Run			Fully Coupled Run				
Model	δH^+(GtC)	δT^+(K)	$\delta CO_2{}^+$(ppm)	δH*(GtC)	δT*(K)	δCO_2*(ppm)	β (GtC ppm^{-1})	γ (GtC K^{-1})
bcc-csm1.1	576.14	0.17	850.54	255.22	3.55	594.93	0.69	−43.07
CanESM2	539.9	0.18	850.54	12.09	5.27	669.43	0.65	−80.50
CESM1-BGC	134.34	0.24	850.54	−112.8	4.03	750.19	0.18	−60.57
FGOALS-s2	37.48	−0.09	850.54	−137.32	5.26	633.95	0.04	−31.02
GFDL-ESM2M	265.76	0.09	288.08	7.43	3.37	592.62	0.98	−169.32
HadGEM2-ES	533.29	0.79	850.54	72.47	4.52	607.8	0.70	−78.02
MPI-ESM-LR	662.43	0.05	850.54	−9.78	4.41	584.95	0.79	−106.35
NorESM1-ME	123.85	0.13	850.54	−126.23	3.67	717.7	0.16	−64.81

[a]Changes of the tropical land carbon pools (δH), tropical near-surface air temperatures (δT) (30°S–30°N), and atmospheric CO_2 concentrations, produced by Earth System Models (ESMs) participating in phase 5 of the Coupled Model Intercomparison Project (CMIP5), and corresponding sensitivities of tropical land carbon sequestrations to the direct CO_2 effect and to climate warming.

The observed tropical mean temperature is derived from the HadCRUT3 data set [*Brohan et al.*, 2006]. Annual mean temperature is calculated following *Cox et al.* [2013]:

$$\overline{T}(n) = \frac{T(n) + T(n-1)}{2}, \tag{4}$$

where $\overline{T}(n)$ denotes the tropical mean temperature centered on the beginning of the nth year. The anomalies of atmospheric CO_2 growth rate and tropical mean temperature are calculated as the residuals of original variations of the time series from the results of the 11 year running mean.

3. Results

3.1. Tropical Land Carbon Concentration and Carbon-Climate Feedback Parameters

In order to obtain the tropical land carbon concentration and carbon-climate feedback parameters, we investigate the changes of tropical temperature, tropical land carbon storage, and atmospheric CO_2 concentration in the eight CMIP5 ESMs (Figure 1). This set of models contains largely the same but not identical models as in some other recent CMIP5 model analyses [*Arora et al.*, 2013; *Friedlingstein et al.*, 2013], due to limitation in model availability for each analysis. The left column shows the results from the fully coupled run and the right column from the biogeochemical coupled run. The simulated atmospheric CO_2 concentration in the emissions-driven fully coupled run (Figure 1c) shows an accelerated increase, mainly caused by anthropogenic emissions (RCP8.5) [*Meinshausen et al.*, 2011] and partially caused by the slowdown of terrestrial carbon uptake, even as a carbon source (Figure 1e). The uncertainty across the ESMs, ranging between 584.95 ppm (MPI-ESM-LR) and 750.19 ppm (CESM1-BGC) (difference between the average of the last 10 years and that of first 10 years; Table 1), results from the various responses of the land and ocean carbon cycle components in each model. The radiative forcing induced by the atmospheric CO_2 concentration will contribute to global warming. The change in tropical temperature (Figure 1a) also shows an accelerated increase, with the range from 3.37 K (GFDL-ESM2M) to 5.27 K (CanESM2). The discrepancy between the atmospheric CO_2 and tropical temperature increase indicates the different climate sensitivities in the ESMs. Tropical terrestrial carbon storage will increase due to strong vegetation photosynthesis via the CO_2 fertilization effect under the high CO_2 concentration and will decrease because of reduced primary productivity owing to the warming temperature as well as regional droughts and enhanced respiration mainly caused by the warming temperature [*Cox et al.*, 2000; *Friedlingstein et al.*, 2006; *Zhao and Running*, 2010]. Figure 1e shows the variations of tropical land carbon storage in ESMs with the increase in temperature and atmospheric CO_2 concentration. Discrepancies occur among the eight ESMs, in that half of them serve as a carbon source in the late 21st century, while the other half remain as a carbon sink. Up to 2099, the strongest release from tropical land carbon storage is −137.32 GtC (FGOALS-s2) and the strongest uptake is 255.22 GtC (bcc-csm1.1).

In the biogeochemical coupled run, the carbon cycle is forced by CO_2 at a rate of a 1% increase per year from the preindustrial value to 4 times that value (Figure 1d) in all but GFDL-ESM2M (in which it increases to double the CO_2 concentration). The atmospheric CO_2 change (850.54 ppm) is stronger than the mean change

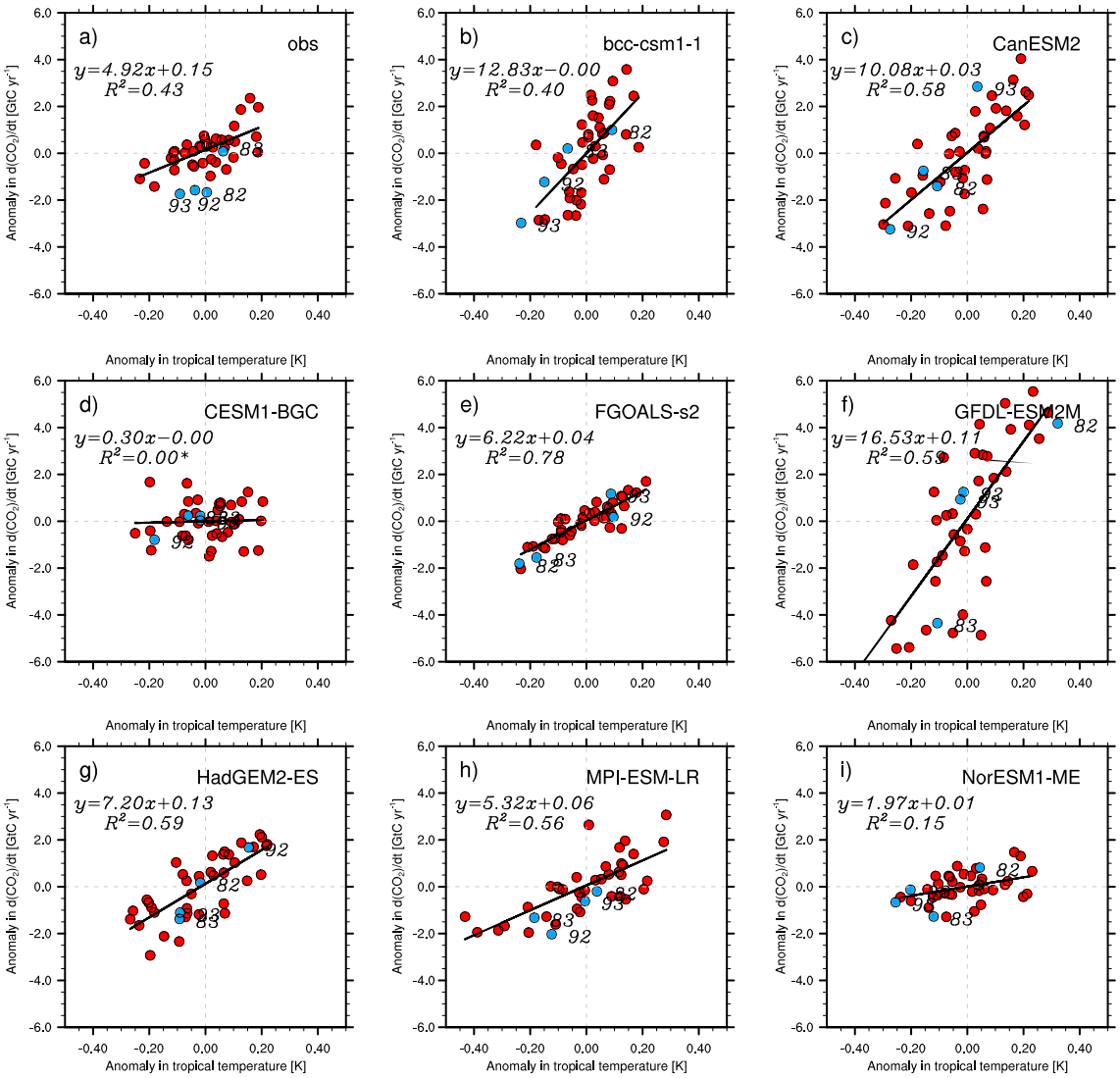

Figure 2. (a–i) The sensitivity of the anomaly in the atmospheric CO_2 growth rate (dCO_2/dt) to the anomaly in tropical near-surface air temperature from 1960 to 2010. The post-volcano years are excluded due to the strong climate perturbations caused by volcanic eruptions (blue dots). The symbol (*) appearing in the coefficient of the determination (R^2) indicates the regression is not significant ($p > 0.05$).

(448.5 ppm) in C^{4}MIP for the uncoupled runs from 1960 to 2099 [*Cox et al.*, 2013]. But the radiation code sees a constant value (284.725 ppm). In the absence of radiative forcing, the tropical temperature shows only a slight increase (Figure 1b), likely due to changes in vegetation structure (leaf area index, vegetation height etc.) and distribution. All models agree that tropical land (Figure 1f) sequesters carbon due to the CO_2 fertilization effect alone. However, the strength of the sequestration is very different, ranging from 37.48 GtC (FGOALS-s2) to 662.43 GtC (MPI-ESM-LR). Nevertheless, the accumulation of tropical carbon storage in the biogeochemical coupled run is significantly stronger than in the fully coupled run. This further suggests the carbon-climate feedback will inhibit the carbon uptake over the tropical land.

We can obtain the sensitivities of the tropical terrestrial carbon concentration and carbon-climate feedbacks (Table 1 and Figure S1) according to equations (1) and (2). The sensitivities of the carbon concentration feedback (β GtC ppm^{-1}) across the ESMs are positive as a result of the enhancement of primary production under CO_2 fertilization, whereas the sensitivities of the carbon-climate feedback (γ GtC K^{-1}) are negative due to the suppressed primary production and increased respiration. Both sensitivities show a large spread. FGOALS-s2 generates the weakest sensitivity of carbon concentration feedback (0.04 GtC ppm^{-1}), while CESM1-BGC and NorESM1-ME have similar magnitudes (0.18 and 0.16 GtC ppm^{-1}) because they both adopt

Table 2. The Interannual Variability From 1960 to 2010[a]

Model	$\sigma(T)$ (K)	$\sigma(dCO_2/dt)$ (GtC yr^{-1})	IAV Sensitivity (GtC yr^{-1} k^{-1})
bcc-csm1.1	0.09	1.75	12.83 ± 2.65
CanESM2	0.14	1.88	10.08 ± 1.46
CESM1-BGC	0.11	0.82	0.30 ± 1.21
FGOALS-s2	0.11	0.81	6.22 ± 0.56
GFDL-ESM2M	0.16	3.37	16.53 ± 2.34
HadGEM2-ES	0.15	1.37	7.20 ± 1.02
MPI-ESM-LR	0.18	1.25	5.32 ± 0.80
NorESM1-ME	0.12	0.6	1.97 ± 0.80
Obs	0.11	0.8	4.92 ± 0.95

[a]The sensitivity of the atmospheric CO_2 annual growth rate to the tropical near-surface air temperature variability from 1960 to 2010. All the calculations exclude post-volcano years (1963, 1964, 1982, 1983, 1992, and 1993) owing to the climate perturbations caused by volcanic eruptions. The second and third columns are the standard deviations of the anomalies in the tropical near-surface air temperature and atmospheric CO_2 annual growth rate, respectively.

the community land model version 4 [*Lawrence et al.*, 2011] as the land component that includes the carbon-nitrogen interactions. The nitrogen limitation [*Thornton et al.*, 2007] can reduce the CO_2 fertilization effect. The sensitivities of carbon concentration feedback in the other ESMs are stronger. On the other hand, the sensitivities of carbon-climate feedback also vary among the ESMs, ranging from −31.02 GtC K^{-1} (FGOALS-s2) to −169.32 GtC K^{-1} (GFDL-ESM2M).

3.2. Interannual Response of Atmospheric CO_2 Growth Rate to Tropical Temperature Variability

The atmospheric CO_2 growth rate shows an unambiguous IAV and a close relationship with tropical temperature variability [*Bacastow*, 1976]. This relationship in the observation and ESMs is presented in Figure 2, with post-volcano years excluded because the climate perturbations induced by volcanic eruptions can alter the IAV of the atmospheric CO_2 growth rate through the diffuse light effect [*Mercado et al.*, 2009]. The standard deviations of anomalies in the atmospheric CO_2 growth rate and tropical temperature are 0.11 K and 0.80 GtC yr^{-1} (Table 2), with the sensitivity being 4.92 ± 0.95 GtC yr^{-1} K^{-1} for the observation (Figure 2a). The IAVs of tropical temperature across the ESMs are comparable to the observation, whereas large uncertainties, from 0.6 GtC yr^{-1} (NorESM1-ME) to 3.37 GtC yr^{-1} (GFDL-ESM2M), occur in the variabilities of the atmospheric CO_2 growth rate (Table 2). Figures 2b–2i show that the sensitivity between the anomaly in the atmospheric CO_2 growth rate and that in tropical temperature varies across the ESMs. In all but two, the sensitivities simulated by the ESMs are higher than in the observation, with the maximum value (16.53 GtC yr^{-1} K^{-1}) in GFDL-ESM2M. These higher sensitivities account for the stronger IAV of the atmospheric CO_2 growth rate in the majority of the ESMs. The sensitivity generated by CESM1-BGC is statistically insignificant, with a value of 0.30 ± 1.21 GtC yr^{-1} K^{-1}, owing to the insignificant dependence of the air-land carbon flux on the tropical mean temperature variability in this model (figure is omitted). The sensitivity in NorESM1-ME also turns out to be relatively weaker (1.97 ± 0.80 GtC yr^{-1} K^{-1}).

3.3. Relationship Between Climate Impact and Sensitivity of the CO_2 Growth Rate

Based on analyses in six general circulation models participating in C^{4}MIP, *Cox et al.* [2013] found a strong linear relationship between the sensitivity of the atmospheric CO_2 growth rate and tropical land carbon-climate feedback parameters, reproduced in Figure 3c. With this model-derived linear relationship, they used the observed sensitivity of the atmospheric CO_2 growth rate to constrain the modeled carbon-climate feedback parameters through the conditional probability approach (see Appendix A). The constraint sharpens the probability density function (PDF) and also, importantly, shifts the mean to a lower value (Figure 3d).

Our analysis with the eight CMIP5 ESMs is shown in Figures 3a and 3b. There is a linear relationship, but it is weak; in fact, it is not statistically significant ($p = 0.25$). As a result, our posterior PDF has nearly the same large spread as the prior PDF. Interestingly, the mean sensitivity shifts to a lower value (Figure 3b), in the same direction of the C^{4}MIP results, albeit much smaller. The differing statistical responses to the sensitivity of atmospheric CO_2 growth rate and tropical land climate impact between C^{4}MIP models and CMIP5 models indicate that the uncertainty in the carbon-climate sensitivity cannot be reduced in the latter set of models using the emergent constraint approach applied by *Cox et al.* [2013] for the former set of models.

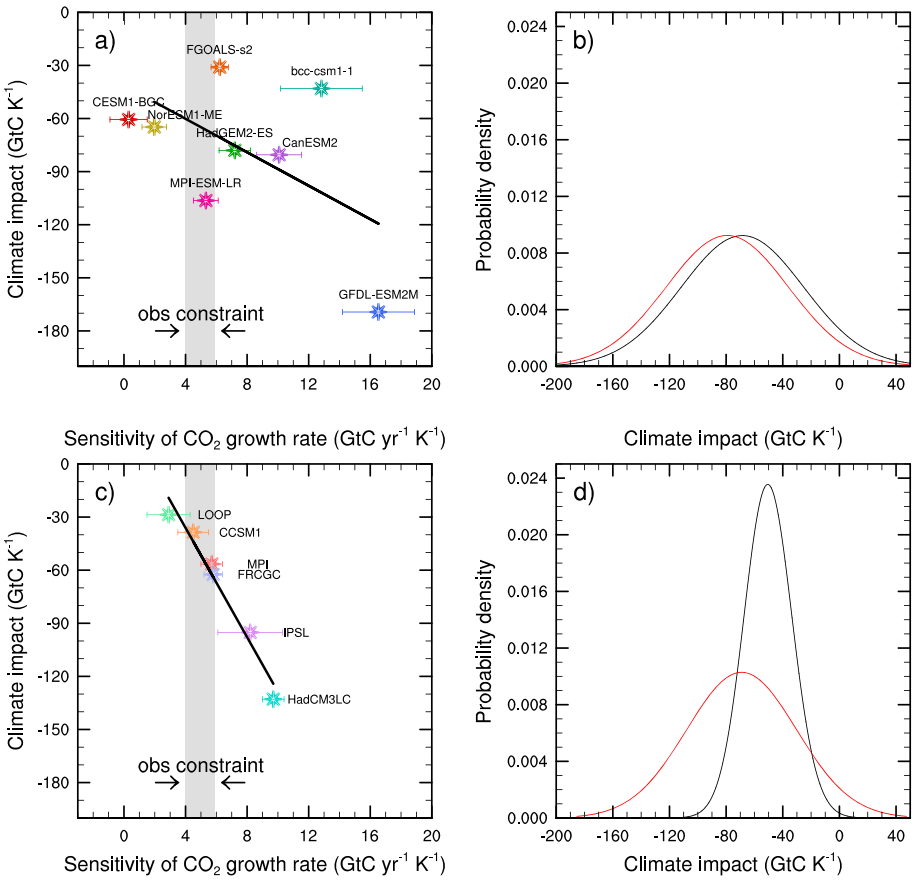

Figure 3. The relationship between the climate impact on tropical land carbon and the sensitivity of the CO_2 growth rate and the emergent constraint on the probability density function (PDF) of the climate impact. (a) Results in the CMIP5 ESMs with an insignificant linear relationship ($p = 0.25$); (c) Coupled Carbon Cycle Climate Model Intercomparison Project (C^4MIP) results with an elegant linear relationship ($p < 0.001$), as shown by *Cox et al.* [2013]. The error bars show the uncertainties in the sensitivity of the CO_2 growth rate, and the gray shaded columns present the observation constraint (4.92 ± 0.95 GtC yr^{-1} K^{-1}). (b, d) A Gaussian distribution of the original climate impact parameters (red solid line) on the basis of an assumption that all the models' results are equally correct (excluding CESM1-BGC owing to the insignificant sensitivity of the CO_2 growth rate in CMIP5); the black solid line denotes the constrained PDF via the relationship between the climate impact and sensitivity of the CO_2 growth rate across the models.

4. Discussion

The magnitude of the carbon-climate or carbon concentration feedback parameters varies with the state of the system, the formulism adopted, the scenario forced, and the specifications of CO_2 from anthropogenic emissions or as atmospheric concentrations [*Boer and Arora*, 2012; *Arora et al.*, 2013]. Besides the fully coupled run, the carbon-climate parameter in *Cox et al.* [2013] is determined by the uncoupled run in which the land and ocean carbon cycles are insensitive to the climate change induced by the Special Report on Emissions Scenarios (SRES) A2 scenario [*Nakicenovic et al.*, 2000] of anthropogenic CO_2 emissions. This uncoupled run is totally different from the biogeochemical run used here to obtain the carbon-climate parameter in the CMIP5 ESMs. Differences in these two runs are as follows: (1) emissions-driven uncoupled run in C^4MIP and concentration-driven biogeochemical run in CMIP5 and (2) the SRES A2 scenario of anthropogenic CO_2 emission in C^4MIP and ideally an increase at a rate of 1% atmospheric CO_2 concentration in CMIP5 (Figure 1d). The forced scenarios and specifications of CO_2 from emissions or prescribed atmospheric concentrations will exert large impacts on the magnitude of the carbon-climate feedback parameter. Besides these differences in the experimental designs, there have to be other potential differences as well, including the models considered, how land use is accounted for, parameterizations across model versions, and so on. These differences may partly explain why the constraint does not emerge in CMIP5 ESMs, while it is significant for the C^4MIP models. Under the limitations in the CMIP5 experimental designs [*Taylor et al.*, 2012], we cannot test the "emergent constraint" of *Cox et al.* [2013] more precisely.

5. Concluding Remarks

In summary, the climate sensitivities of tropical land carbon in CMIP5 ESMs are all negative, suggesting that the temperature warming alone will make tropical land release carbon into the atmosphere. The majority of the sensitivities of the atmospheric CO_2 growth rate to tropical mean temperature are stronger in the ESMs than in the modern observations. Unlike the earlier C^4MIP models, there is only a weak linear relationship ($p = 0.25$). As a result, the uncertainty of climate impact in the CMIP5 ESMs can barely be reduced using the constraining approach of *Cox et al.* [2013]. Besides such model dependence, physical considerations also suggest that some processes involving longer-term adjustment in, for example, photosynthesis, nitrogen limitation, soil turnover, and tree demographic responses may not manifest themselves on interannual time scales [*Zeng et al.*, 2004; *Matthews et al.*, 2005; *Hungate et al.*, 2013; *Friend et al.*, 2014]. Reversely, these processes make the carbon cycle biases persist on decadal time scales [*Hoffman et al.*, 2014]. Therefore, it remains a major challenge to use modern observations to constrain future carbon cycle responses and interaction with climate. Scientifically, these emergent constraints must be continuously evaluated to determine how well they hold as results from new model intercomparison experiments become available.

Appendix A: Linear Least Squares Fitting and the PDF Method for Carbon-Climate Impact (γ)

The linear least squares fitting is the simplest and most commonly applied technique. For a linear fit, $y_i = a + bx_i + \varepsilon_i$, where a and b denote the intercept with the y axis and the gradient, respectively. The x_i and y_i are the two series. The ε_i denotes the error between the actual vertical point, y_i, and the fitting point, ($\varepsilon_i = y_i - \hat{y}_i$). Let

$$\left.\begin{aligned} SS_{xx} &= \sum_{i=1}^{n}(x_i - \overline{x}), \\ SS_{yy} &= \sum_{i=1}^{n}(y_i - \overline{y}), \\ SS_{xy} &= \sum_{i=1}^{n}(x_i - \overline{x})\,(y_i - \overline{y}). \end{aligned}\right\},$$

where $\overline{x}$ and $\overline{y}$ denote the mean of the time series.

According to the maximum likelihood estimation, the regression coefficient $\hat{b} = SS_{xy}/SS_{xx}$, and $\hat{a}$ is given in terms of $\hat{a} = \overline{y} - \hat{b}\overline{x}$. We define s^2 as an estimator for the variance in ε_i,

$$s^2 = \sum_{i=1}^{n}\frac{\varepsilon_i^2}{n-2} = \frac{SS_{yy} - SS_{xy}^2/SS_{xx}}{n-2}.$$

The standard error for $\hat{b}$ is given as $\sigma_b = s/\sqrt{SS_{xx}}$, which defines a Gaussian probability density for $\hat{b}$:

$$P\left(\hat{b}\right) \sim N\left(b, \sigma_b^2\right).$$

The prediction error at $x - x_i$ is given as

$$P\left(\hat{Y} - f(x_i)\right) \sim N\left(0, \left[1 + \frac{1}{n} + \frac{(x_i - \overline{x})^2}{SS_{xx}}\right]s^2\right).$$

Let $\sigma_f^2 = \left[1 + \frac{1}{n} + \frac{(x-\overline{x})}{SS_{xx}}\right]s^2$; the probability density of $\hat{Y}$ given x is

$$P\left(\hat{Y}|x\right) \sim N\left(f(x), \sigma_f^2\right).$$

Because of the emergent significant linear relationship between the carbon-climate feedback parameter of tropical land carbon sequestrations (γ_{LT}) and the sensitivity of historical atmospheric CO_2 growth rate to tropical temperature variability (γ_{CO_2}) in *Cox et al.* [2013], we can deduce the probability density of γ_{LT} given γ_{CO_2}, namely, $P\left(\gamma_{LT}|\gamma_{CO_2}\right)$. Additionally, the linear relationship between the observed annual anomalies in the atmospheric CO_2 growth rate and the tropical mean temperature provides the observation-based probability density of γ_{CO_2}, and so

$$P(\gamma_{LT}) = \int_{-\infty}^{\infty} P\left(\gamma_{LT}|\gamma_{CO_2}\right) P\left(\gamma_{CO_2}\right) \mathrm{d}\gamma_{CO_2}.$$

Acknowledgments

The data of the ESMs in CMIP5 are supported by the U.S. Department of Energy's Program for Climate Model Diagnosis and Intercomparison. The global marine surface annual mean CO_2 data are from the NOAA website, and the CO_2 from the Representative Concentration Pathway are from Potsdam Institute for Climate Impact Research. The tropical surface temperatures are available at the CRU/Met Office. We are grateful for the thorough review by two anonymous reviewers. This work was supported by the Chinese Academy of Sciences (XDA05110303 and XDA11010402), the "973" projects (2010CB950404 and 2013CB955803), NSFC (Grant Nos. 91337110 and 41023002).

The Editor thanks two anonymous reviewers for their assistance in evaluating this paper.

References

Andres, R. J., J. S. Gregg, L. Losey, G. Marland, and T. A. Boden (2011), Monthly, global emissions of carbon dioxide from fossil fuel consumption, *Tellus B*, *63*(3), 309–327, doi:10.1111/j.1600-0889.2011.00530.x.

Arora, V. K., J. F. Scinocca, G. J. Boer, J. R. Christian, K. L. Denman, G. M. Flato, V. V. Kharin, W. G. Lee, and W. J. Merryfield (2011), Carbon emission limits required to satisfy future representative concentration pathways of greenhouse gases, *Geophys. Res. Lett.*, *38*, L05805, doi:10.1029/2010GL046270.

Arora, V. K., et al. (2013), Carbon-concentration and carbon–climate deedbacks in CMIP5 Earth System Models, *J. Clim.*, *26*(15), 5289–5314, doi:10.1175/jcli-d-12-00494.1.

Bacastow, R. B. (1976), Modulation of atmospheric carbon dioxide by the Southern Oscillation, *Nature*, *261*, 116–118, doi:10.1038/261116a0.

Bao, Q., et al. (2013), The Flexible Global Ocean-Atmosphere-Land system model, Spectral Version 2: FGOALS-s2, *Adv. Atmos. Sci.*, *30*(3), 561–576, doi:10.1007/S00376-012-2113-9.

Boer, G. J., and V. K. Arora (2012), Feedbacks in emission-driven and concentration-driven global carbon budgets, *J. Clim.*, *26*(10), 3326–3341, doi:10.1175/JCLI-D-12-00365.1.

Booth, B. B. B., C. D. Jones, M. Collins, I. J. Totterdell, P. M. Cox, S. Sitch, C. Huntingford, R. A. Betts, G. R. Harris, and J. Lloyd (2012), High sensitivity of future global warming to land carbon cycle processes, *Environ. Res. Lett.*, *7*(2), 024002, doi:10.1088/1748-9326/7/2/024002.

Brohan, P., J. J. Kennedy, I. Harris, S. F. B. Tett, and P. D. Jones (2006), Uncertainty estimates in regional and global observed temperature changes: A new data set from 1850, *J. Geophys. Res.*, *111*, D12106, doi:10.1029/2005JD006548.

Collins, W. J., et al. (2011), Development and evaluation of an Earth-System model-HadGEM2, *Geosci. Model Dev.*, *4*(4), 1051–1075, doi:10.5194/Gmd-4-1051-2011.

Cox, P. M., R. A. Betts, C. D. Jones, S. A. Spall, and I. J. Totterdell (2000), Acceleration of global warming due to carbon-cycle feedbacks in a coupled climate model, *Nature*, *408*, 184–187.

Cox, P. M., R. A. Betts, M. Collins, P. P. Harris, C. Huntingford, and C. D. Jones (2004), Amazonian forest dieback under climate-carbon cycle projections for the 21st century, *Theor. Appl. Climatol.*, *78*(1-3), 137–156, doi:10.1007/s00704-004-0049-4.

Cox, P. M., D. Pearson, B. B. Booth, P. Friedlingstein, C. Huntingford, C. D. Jones, and C. M. Luke (2013), Sensitivity of tropical carbon to climate change constrained by carbon dioxide variability, *Nature*, *494*(7437), 341–344, doi:10.1038/nature11882.

Dufresne, J. L., P. Friedlingstein, M. Berthelot, L. Bopp, P. Ciais, L. Fairhead, H. Le Treut, and P. Monfray (2002), On the magnitude of positive feedback between future climate change and the carbon cycle, *Geophys. Res. Lett.*, *29*(10), 1405, doi:10.1029/2001GL013777.

Dunne, J. P., et al. (2013), GFDL's ESM2 Global Coupled Climate-Carbon Earth System Models. Part II: Carbon system formulation and baseline simulation characteristics, *J. Clim.*, *26*(7), 2247–2267, doi:10.1175/Jcli-D-12-00150.1.

Friedlingstein, P., J. L. Dufresne, P. M. Cox, and P. Rayner (2003), How positive is the feedback between climate change and the carbon cycle?, *Tellus*, *55B*, 692–700.

Friedlingstein, P., et al. (2006), Climate-carbon cycle feedback analysis: Results from the C^4MIP model intercomparison, *J. Clim.*, *19*(14), 3337–3353, doi:10.1175/jcli3800.1.

Friedlingstein, P., M. Meinshausen, V. K. Arora, C. D. Jones, A. Anav, S. K. Liddicoat, and R. Knutti (2013), Uncertainties in CMIP5 climate projections due to carbon cycle feedbacks, *J. Clim.*, *27*, 511–526, doi:10.1175/jcli-d-12-00579.1.

Friend, A. D., et al. (2014), Carbon residence time dominates uncertainty in terrestrial vegetation responses to future climate and atmospheric CO_2, *Proc. Natl. Acad. Sci. U.S.A.*, *111*(9), 3280–3285, doi:10.1073/pnas.1222477110.

Hoffman, F. M., et al. (2014), Causes and implications of persistent atmospheric carbon dioxide biases in Earth System Models, *J. Geophys. Res. Biogeosci.*, *119*, 141–162, doi:10.1002/2013JG002381.

Houghton, R. A. (2010), How well do we know the flux of CO_2 from land-use change?, *Tellus Ser. B Chem. Phys. Meteorol.*, *62*(5), 337–351, doi:10.1111/J.1600-0889.2010.00473.X.

Hungate, B. A., P. Dijkstra, Z. T. Wu, B. D. Duval, F. P. Day, D. W. Johnson, J. P. Megonigal, A. L. P. Brown, and J. L. Garland (2013), Cumulative response of ecosystem carbon and nitrogen stocks to chronic CO_2 exposure in a subtropical oak woodland, *New Phytol.*, *200*(3), 753–766, doi:10.1111/Nph.12333.

Huntingford, C., et al. (2013), Simulated resilience of tropical rainforests to CO_2-induced climate change, *Nat. Geosci.*, *6*, 268–273, doi:10.1038/ngeo1741.

Hurrell, J. W., et al. (2013), The Community Earth System Model: A framework for collaborative research, *Bull. Am. Meteorol. Soc.*, *94*(9), 1339–1360, doi:10.1175/Bams-D-12-00121.1.

Ilyina, T., K. D. Six, J. Segschneider, E. Maier-Reimer, H. M. Li, and I. Nunez-Riboni (2013), Global ocean biogeochemistry model HAMOCC: Model architecture and performance as component of the MPI-Earth system model in different CMIP5 experimental realizations, *J. Adv. Model Earth Syst.*, *5*(2), 287–315, doi:10.1029/2012MS000178.

Jones, C. D., et al. (2011), The HadGEM2-ES implementation of CMIP5 centennial simulations, *Geosci. Model Dev.*, *4*(3), 543–570, doi:10.5194/Gmd-4-543-2011.

Keppel-Aleks, G., et al. (2013), Atmospheric carbon dioxide variability in the Community Earth System Model: Evaluation and transient dynamics during the twentieth and twenty-first centuries, *J. Clim.*, *26*(13), 4447–4475, doi:10.1175/jcli-d-12-00589.1.

Lawrence, D. M., et al. (2011), Parameterization improvements and functional and structural advances in version 4 of the Community Land Model, *J. Adv. Model Earth Syst.*, *3*, M03001, doi:10.1029/2011MS000045.

Marengo, J. A., C. A. Nobre, J. Tomasella, M. D. Oyama, G. Sampaio de Oliveira, R. de Oliveira, H. Camargo, L. M. Alves, and I. F. Brown (2008), The drought of Amazonia in 2005, *J. Clim.*, *21*(3), 495–516, doi:10.1175/2007jcli1600.1.

Marengo, J. A., J. Tomasella, L. M. Alves, W. R. Soares, and D. A. Rodriguez (2011), The drought of 2010 in the context of historical droughts in the Amazon region, *Geophys. Res. Lett.*, *38*, L12703, doi:10.1029/2011GL047436.

Matthews, H. D., M. Eby, A. J. Weaver, and B. J. Hawkins (2005), Primary productivity control of simulated carbon cycle-climate feedbacks, *Geophys. Res. Lett.*, *32*, L14708, doi:10.1029/2005GL022941.

Meinshausen, M., et al. (2011), The RCP greenhouse gas concentrations and their extensions from 1765 to 2300, *Clim. Change*, *109*(1–2), 213–241, doi:10.1007/S10584-011-0156-Z.

Mercado, L. M., N. Bellouin, S. Sitch, O. Boucher, C. Huntingford, M. Wild, and P. M. Cox (2009), Impact of changes in diffuse radiation on the global land carbon sink, *Nature*, *458*(7241), 1014–U1087, doi:10.1038/Nature07949.

Nakicenovic, N., et al. (2000), Emissions scenarios: Summary for policymakers, *Spec. Report* (Intergovernmental Panel on Climate Change, 2000).

Phillips, O. L., et al. (2009), Drought sensitivity of the Amazon rainforest, *Science*, *323*(5919), 1344–1347, doi:10.1126/Science.1164033.

Riahi, K., A. Grübler, and N. Nakicenovic (2007), Scenarios of long-term socio-economic and environmental development under climate stabilization, *Technol. Forecasting Social Change*, *74*(7), 887–935, doi:10.1016/j.techfore.2006.05.026.

Shao, P., X. B. Zeng, K. Sakaguchi, R. K. Monson, and X. D. Zeng (2013), Terrestrial carbon cycle: Climate relations in eight CMIP5 Earth System Models, *J. Clim.*, *26*(22), 8744–8764, doi:10.1175/JCLI-D-12-00831.1.

Taylor, K. E., R. J. Stouffer, and G. A. Meehl (2012), An overview of CMIP5 and the experiment design, *Bull. Am. Meteorol. Soc.*, *93*(4), 485–498, doi:10.1175/Bams-D-11-00094.1.

Thornton, P. E., J. F. Lamarque, N. A. Rosenbloom, and N. M. Mahowald (2007), Influence of carbon-nitrogen cycle coupling on land model response to CO_2 fertilization and climate variability, *Global Biogeochem. Cycles*, *21*, Gb4018, doi:10.1029/2006GB002868.

Tjiputra, J. F., C. Roelandt, M. Bentsen, D. M. Lawrence, T. Lorentzen, J. Schwinger, Ø. Seland, and C. Heinze (2012), Evaluation of the carbon cycle components in the Norwegian Earth System Model (NorESM), *Geosci. Model Dev. Discuss.*, *5*(4), 3035–3087, doi:10.5194/gmdd-5-3035-2012.

Wang, J., Q. Bao, N. Zeng, Y. M. Liu, G. X. Wu, and D. Y. Ji (2013), Earth System Model FGOALS-s2: Coupling a dynamic global vegetation and terrestrial carbon model with the physical climate system model, *Adv. Atmos. Sci.*, *30*(6), 1549–1559, doi:10.1007/S00376-013-2169-1.

Wu, T. W., et al. (2013), Global carbon budgets simulated by the Beijing Climate Center Climate System Model for the last century, *J. Geophys Res. Atmos.*, *118*, 4326–4347, doi:10.1002/Jgrd.50320.

Zeng, N., H. F. Qian, E. Munoz, and R. Iacono (2004), How strong is carbon cycle-climate feedback under global warming?, *Geophys. Res. Lett.*, *31*, L20203, doi:10.1029/2004GL020904.

Zeng, N., J.-H. Yoon, J. A. Marengo, A. Subramaniam, C. A. Nobre, A. Mariotti, and J. D. Neelin (2008), Causes and impacts of the 2005 Amazon drought, *Environ. Res. Lett.*, *3*(1), 014002, doi:10.1088/1748-9326/3/1/014002.

Zhao, M., and S. W. Running (2010), Drought-induced reduction in global terrestrial net primary production from 2000 through 2009, *Science*, *329*(5994), 940–943, doi:10.1126/science.1192666.